



# HHS Public Access

## Author manuscript

*Appl Radiat Isot.* Author manuscript; available in PMC 2022 September 01.

Published in final edited form as:

*Appl Radiat Isot.* 2021 September ; 175: 109824. doi:10.1016/j.apradiso.2021.109824.

## Rapid HPGe Well Detector Gamma Bioassay of $^{137}\text{Cs}$ , $^{60}\text{Co}$ , and $^{192}\text{Ir}$ Method

**Jonathan Button\***, **Robert L. Jones**

Inorganic and Radiation Analytical Toxicology Branch, Centers for Disease Control and Prevention, 4770 Buford Highway, Mail Stop S103-1, Atlanta, GA 30341, USA

### Abstract

CDC designed a rapid HPGe Bioassay Method for  $^{137}\text{Cs}$ ,  $^{60}\text{Co}$ , and  $^{192}\text{Ir}$  that is suitable for a public health response to a radiological incident where people may ingest or inhale radionuclides. The method uses a short count time, small sample volume, and a large volume detector and well size. It measures a patient's urine sample collected post-incident. The levels of concern are directly related to the Clinical Decision Guide levels recommended in the National Council of Radiation Protection 161.

### Keywords

$^{137}\text{Cs}$ ;  $^{60}\text{Co}$ ;  $^{192}\text{Ir}$ ; HPGe; urine; emergency response

### Introduction

CDC has developed rapid analytical methods for screening and quantifying radionuclides in samples of human urine to be able to respond to a significant radiological or nuclear incident. Health officials or health physicists may use the measurement of activity to evaluate internal contamination and estimate radioactive dose to individuals during and following a radiological or nuclear incident. In some past emergency incidents involving toxins or radionuclides, responders and health officials found a need to screen or test on the order of hundreds of thousands of individuals. Often, only a small number of individuals will actually be contaminated requiring medical follow-up, relative to the large number of people that will need or request screening or testing for contamination or exposure. An accurate measure of internal and external exposure and contamination is critical for the effective treatment of those exposures and contaminations as well as for the successful containment of radiological contamination. (Dörr and Meineke, 2006)

\* Author to whom correspondence should be addressed: jbutton@cdc.gov; Fax: +1 770 488 4097; Tel: +1 404 498 1550.

**Publisher's Disclaimer:** The findings and conclusions in this study are those of the authors and do not necessarily represent the views of the US Department of Health and Human Services or the Centers for Disease Control and Prevention. The use of trade names and commercial sources is for identification only and does not constitute an endorsement by the US Department of Health and Human Services or the Centers for Disease Control and Prevention.

**Conflict of interest:** The authors declare that they have no competing interests.

The National Council of Radiation Protection in NCRP 161 created the concept of Clinical Decision Guide (CDG) levels. At certain levels of acute radiation dose, a patient may experience no deterministic effect but will suffer from a significant and quantifiable increase in stochastic lifetime (50 years) risk of cancer or tumor formation (Keith et al., 1999; National Council on Radiation Protection and Measurements, 2009; Obodovskiy, 2015; Schull and Weiss, 1992). “Deterministic” and “stochastic” refer to effects that are definitively caused by radiation exposure in the former case or effects where the causality is inferred or challenging to determine in the latter case. Using the methodology in NCRP 161, the CDC calculated the Children or Pregnant Women (C/P) CDG values (Table 1) for the activity concentration (Bq/L) of a patient sample at varying numbers of days post-exposure and different radionuclides of interest. The CDG C/P value is one-fifth of the Adult CDG value. NCRP states that one CDG level corresponds to a 1.3% lifetime increased risk of stochastic effects. As shown in Table 1, the Limits of Detection (LOD) for radionuclide measurements validated for this method are orders of magnitude below the C/P CDG levels.

The analytical method uses well geometry High Purity Germanium (HPGe) detectors with a nominal active volume of 450 cubic centimeters. We optimized the measurement parameters to our requirements. The requirements are appropriate for a laboratory method that provides reportable clinical results to aid the emergency response effort following a radiological incident. In order to make the method rapid, we use a relatively short live count time of 15 minutes. The high counting efficiency of well geometry HPGe detectors allows us to use a small sample volume of 10 mL. The small sample volume is simpler to collect and ship than a 24-hr urine sample during a Public Health incident response. The detector well is relatively large and can accommodate a 15 mL centrifuge tube, a sample container which is easy to stockpile. We obtain the efficiency calibration via the True Cascade Correction (TCC) polynomial fit and correction method in ORTEC’s GammaVision software. This efficiency calibration method gives us flexibility in terms of adding radionuclides to the method in the future. We validated the method according to CLIA regulations and the FDA Bioanalytical Guidance (Center for Drug Evaluation and Research and Center for Veterinary Medicine, 2018) for accuracy, precision, the limit of detection, linearity, specificity, stability, and robustness.

CDC validated the method for the identification and quantification of  $^{137}\text{Cs}$ ,  $^{60}\text{Co}$ , and  $^{192}\text{Ir}$  as well as  $^{131}\text{I}$ ,  $^{75}\text{Se}$ , and  $^{99}\text{Mo}$  in human patient samples. This paper will focus on the former group of analytes, as they represent a progression from relatively simple-to-complex in terms of identification and quantification by HPGe spectrometry.  $^{137}\text{Cs}$  measurement is unaffected by cascade summing. Cascade summing complicates  $^{60}\text{Co}$  measurement by causing count losses to its two gamma peaks. Similarly, cascade summing losses appear in multiple gamma peaks for  $^{192}\text{Ir}$  measurement.

### Gamma Screen

The CDC Urine Radionuclide Screen is a set of analytical methods that rapidly identify higher than background levels of radioactivity in a 0.5 to 10 mL sample from a 30–50 mL spot collection of patient urine. A NaI method screens for gamma emitters with a 5-minute count time. The gamma screen method uses NaI well detectors to measure the activity as an

integral count over the same energy span as the HPGe method (50–2000 keV) in a 10 mL sample of patient urine held in a 15 mL centrifuge tube. For a sample that indicates an elevated activity level above a population background, we forward the sample to the HPGe method, which measures the same tube and sample for specific radionuclide activity. We established the background level by measurement of 100 individual samples of non-contaminated urine.

### High Purity Germanium (HPGe) Detector System Description

Five p-type reverse coaxial well HPGe detector systems are currently in operation for this method but with the capacity and plans to expand to six detectors. They are all ORTEC/AMETEK detector systems and have a nominal active detector volume of 450 cubic centimeters. Each well can accommodate a 15 mL polypropylene tube (see Figure 1). This sample-detector geometry has a very high counting efficiency and allows for a small sample size. Drawbacks for this sample-detector geometry include a larger energy resolution (as compared to a conventional coaxial geometry) as well as significant summing effects.

### Method Analytes

**<sup>137</sup>Cs**—<sup>137</sup>Cs is a beta and gamma emitter. In gamma spectroscopy, it is easily identified and quantified by the 661 keV gamma decay of the daughter product <sup>137</sup>Ba, which accompanies 85% of <sup>137</sup>Cs decays (Bé and Bureau International des Poids et Mesures, 2013). This analyte is significant from a public health perspective in that it has been present in one-fifth of the radiological incidents tracked by the Nuclear Regulatory Commission (NRC). (National Council on Radiation Protection and Measurements, 2009) <sup>137</sup>Cs is a fission product. Nuclear weapon detonations and nuclear power plant accidents are common routes for <sup>137</sup>Cs to enter the environment. Releases to the environment may also follow the theft or loss of a <sup>137</sup>Cs source used for irradiation or imaging.

Fear of widespread contamination by <sup>137</sup>Cs followed the Goiania incident (E. Toohey, 2003) in 1987. Misleading media reports following the incident spread fears of possible widespread contamination, and as a result, officials screened over 112,000 individuals for contamination. Of that number, 46 patients would receive treatment for internal contamination. For the first time following a radiological incident, clinicians prescribed Prussian Blue as a decontamination treatment for patients suffering from internal contamination of <sup>137</sup>Cs. The therapy reduced the effective biological half-life from 63 days in females and 89 days in males to an average of 29 days. (E. Toohey, 2003) Health officials may use data from a rapid and accurate assessment of <sup>137</sup>Cs internal contamination to aid decisions for prioritizing Prussian Blue usage in similar incidents.

**<sup>60</sup>Co**—NCRP 161 and the ATSDR toxicological profile for Cobalt review common routes of exposure to <sup>60</sup>Co and its public health significance. <sup>60</sup>Co is an activation product produced by bombardment of stable <sup>59</sup>Co with neutrons. Inhalation is a primary route for internal contamination and exposure, particularly in nuclear workers around reactors, fuel reprocessing sites, and waste management sites. <sup>60</sup>Co has applications in medical therapies, gamma sterilization, and industrial radiography. When an individual inhales <sup>60</sup>Co, it may remain in the lungs for a very long time, with biological half-lives on the order of 1.5 to 17

years seen in individual cases. The human body retains  $^{60}\text{Co}$  mainly in the liver, kidneys, and bones.

**$^{192}\text{Ir}$** — $^{192}\text{Ir}$  is a beta and gamma emitter. In brachytherapy, a doctor implants a sealed  $^{192}\text{Ir}$  source into a body cavity near a cancerous tumor site. The source delivers an effective radiation dose directly to the target cells. Industrial radiography applications with a  $^{192}\text{Ir}$  source include identifying flaws in a metal casting or a weld.  $^{192}\text{Ir}$  is not as prevalent as  $^{137}\text{Cs}$  or  $^{60}\text{Co}$ . However, NCRP 161(National Council on Radiation Protection and Measurements, 2009) does point out two specific case studies. In one, a harmful dose of  $^{192}\text{Ir}$  was accidentally inhaled by two workers who were cutting into a capsule containing  $^{192}\text{Ir}$  pellets. In the other, workers absorbed a harmful dose of  $^{192}\text{Ir}$  through the skin after incorrectly mixing  $^{192}\text{Ir}$  with toluene and causing an explosion. In the inhalation case, the analysis of  $^{192}\text{Ir}$  activity in urine had limited usefulness in dose assessment because of the long bio-half-life of  $^{192}\text{Ir}$  in the lungs (greater than 1,000 days). The biological half-life depends on the chemical form of  $^{192}\text{Ir}$ .

## Detector Calibration

We obtain the HPGe calibration using the calibration wizard method internal to the ORTEC GammaVision software (ORTEC, 2017). The wizard performs three separate calibrations (energy, full-width half-maximum energy resolution, and efficiency) and will perform one or two corrections to the efficiency calibration to account for cascade summing effects. The first correction is the Peak-to-Total Ratio (Blaauw, 1993), and the second is the Linear-to-Square Ratio (Gelsema, 2001). The energy and full-width half-maximum energy resolution calibrations are both required for accurate and precise identification of peaks using the software's built-in peak search algorithm. The software matches identified peak energies within a given spectrum to the energies in a user-defined library of radionuclides of interest and their associated x- or gamma-rays. The efficiency is the probability that a photon emission from the measured source will appear as a count in the full-energy peak (FEP) for that photon energy. The software calculates and reports an activity based on branching ratio (BR%) unique to the identified radionuclide and photon energy, the efficiency, and the observed count-rate within the full-energy peak.

We calibrated each detector system with a single True Cascade Correction (TCC) mixture calibrator solution (Eckert & Ziegler Analytics SRS#114539). The radioactive source is 10 mL of solution in a 15 mL centrifuge tube or the same geometry used in the method. Decay corrected values for the activity of each of the radionuclides present in the solution (11) are in Table 2. The certificate date and time are for 8/1/2019 12:00:00 PM, and the certified activities are NIST-traceable.

## Method Validation

We obtained the method validation data by performing sample measurements in analytical runs unless otherwise specified. An analytical run is sample measurements bracketed by quality control measurements. Lab policy specifies that analytical runs may not last longer than 24 hours. At each step in the method development and validation process, we chose

sample target activities that match a range of CDG values. These target selections ensure that the method validation data we obtained is relevant for the method purpose.

## Accuracy

The laboratory policy for all analytical methods is that mean concentration after ten individual measurements in ten separate analytical runs should be within 15% of the nominal characterized target value. If the nominal value is equal to or less than three times the method's limit of detection, then the mean activity should be within 20% of the nominal value. This approach to evaluating the method accuracy is aligned with regulations for clinical lab method

For each radionuclide, we prepared three sets of dilutions of NIST material (in the case of  $^{60}\text{Co}$ ) or NIST-traceable reference materials (for  $^{137}\text{Cs}$  and  $^{192}\text{Ir}$ ) (Table 3) to determine method accuracy. We pipetted the appropriate amount of standard source solution into the sample and then verified that amount by mass measurement. We then calculated the reference activity levels shown in Table 4 from the mass measurement data. The uncertainties of the reference activity levels include the expanded uncertainties from the source solution certificate and the uncertainties of the mass measurements made during the dilution steps.

For  $^{137}\text{Cs}$ , we targeted activity concentrations to range from one-third the C/P 5-day CDG value to 2x the Adult 5-day CDG value. The accuracy of measurements over the range is within 3% of reference values. For  $^{60}\text{Co}$ , we targeted activity concentrations to range from 1x the Adult 1-day CDG value to 8x the Adult 5-day CDG value. The accuracy of measurements over the range is within 2% of reference values. For  $^{192}\text{Ir}$ , we targeted activity concentrations to range from 1x the C/P 1-day CDG value to 4x the Adult 1-day CDG value. The accuracy of measurements over the range is within 6% of reference values. The difference between the reference and mean values for all radionuclides are well within the lab's  $\pm 15\%$  limit.

In order to evaluate the method accuracy more thoroughly, we considered the uncertainties of the reference values and measurement values by calculating z-score. The uncertainties for the mean measurements in Table 4 include standard deviation and the uncertainties related to detection efficiency and peak areas. The z-score at each activity level is calculated using

$$z = \frac{\mu_{\text{meas}} - X_{\text{ref}}}{\sqrt{\sigma_{\text{meas}}^2 + \sigma_{\text{ref}}^2}}, \text{ where } \mu_{\text{meas}} \text{ is the mean measurement, } X_{\text{ref}} \text{ is the reference value, and } \sigma$$

are the uncertainties related to the measurement and the reference value. For both  $^{137}\text{Cs}$  and  $^{60}\text{Co}$ , the mean value at each activity level is in good agreement with the reference value. For  $^{192}\text{Ir}$ , mean and reference values are within  $2\sigma$  uncertainty of each other. The uncertainties for the mean measurements in Table 4 include standard deviation and the uncertainties related to detection efficiency and peak areas. We conclude the reference values and mean values are in good agreement for all the sample data shown in Table 4.

The TCC mixture that we use does not include  $^{60}\text{Co}$  or  $^{192}\text{Ir}$ , so we may conclude that these results confirm the accuracy of the calibration model (Blaauw, 1993; Gelsema, 2001; Gunnink and Prindle, 1992; ORTEC, 2017) in the ORTEC GammaVision calibration wizard.

## Precision

Precision is the closeness of individual repeat measurements of an analyte. The laboratory policy is that the total relative standard deviation should be less than 15%. We prepared samples at two activity levels for each radionuclide for precision tests. The method precision comes out of a comparison of measurement results at both levels across 20 measurements and over ten analytical runs. We distributed these analytical runs across four instruments.

The aggregated precision data is in Table 5, with precision results shown as the standard deviation across the ten analytical runs (the Between-Run standard deviation) and as the standard deviation across the two measurements taken in the same analytical run (the Within-Run standard deviation). Between-Run precision ranges from 2–10x larger than the Within-Run precision, and this difference is primarily due to variation between instruments. In Figure 6, the different shapes and colors of the data points represent the four instrument systems. Visual inspection of the figures shows a clear detector bias in both <sup>137</sup>Cs samples and in Co60-QC-H and no detector bias in the other samples.

## Sensitivity/Limit of Detection

The Limit of Detection (LOD) is the lowest concentration at which the method can detect an analyte in the sample with a defined probability. The probability adopted by the CDC radiation lab is  $\sim\pm100\%$  at a 95% confidence interval. The LOD is used for method validation rather than the Minimum Detectable Activity (MDA) because LOD is the preferred method parameter by clinical laboratories. We have experimentally measured the LOD by relating the average activities and standard deviation for at least four low activity level samples and one blank sample across a minimum of 20 measurements. (CLSI, 2012; Taylor, 1987)

The activity concentration measurement data for these samples are analyzed in a custom SAS program by a lab statistician. The program calculates the LOD from this data for different scenarios: varying the number of samples admitted into the model, varying the fit model (average, linear, and quadratic) to the mean vs. variance data, and varying the LOD calculation method (Taylor and Clinical & Laboratory Standards Institute (CLSI)). The software checks assumptions about the distributions of blank and low activity sample measurements by providing both the parametric and nonparametric estimates of mean and 95<sup>th</sup> percentile results. The LOD values are judged by their associated statistical test and by giving qualitative grades to the goodness-of-fit of the variance vs. mean data. We show the best fit scenarios for each of the radionuclides in Figure 2. The LOD values determined are shown in Table 1.

## Linearity

In HPGe gamma spectroscopy, the instrument linearity is guaranteed by the manufacturer over a potentially limitless range of activities and radionuclides. However, we do not assume familiarity with HPGe instrumentation on the part of clinical lab regulators, public health policy decision makers, or medical doctors who may use results from this method to guide patient care. Therefore, we have applied a method of assessing linearity that is generic to clinical lab methods and is prescribed by our laboratory policy. Furthermore, by lab policy,

we may only report clinical results for measurements within the linear range that we have validated experimentally.

Linearity may be interpreted to mean that the relationship is linear between the raw instrument signal and the expected measurement result. Often this is not the case, and instead, the linearity can be assessed from the relationship between the final measurement result and the expected result. The HPGe efficiency calibration model adopted in this method shows that the raw instrument signal (observed counts in a full-energy peak) is linear with radionuclide activity but is non-linear with the gamma energy. Furthermore, the detector response depends on the emitting nuclide via cascade summing. Therefore, we assess the linearity for this method by comparing the average vs. expected activity concentrations. The linearity data (Figure 3) is from measurement results for a minimum of 5 samples per radionuclide and 20 measurements per sample.

The CDC laboratory requirement is that the linear fit between average measurement and expected measurement must have a coefficient of determination ( $R^2$ ) greater than 0.98. Additionally, the laboratory requires that the residual regression plot show no curvilinear relationship between the expected measurement and the residual. As a final check, the quadratic term from the quadratic regression of the same data must not be statistically significant with  $P < .05$ . The  $^{137}\text{Cs}$ ,  $^{60}\text{Co}$ , and  $^{192}\text{Ir}$  data shown in Figure 3 meet our linearity requirements. We consider the method to be linear up to and including the maximum linear activity concentrations shown in Table 6.

### Maximum Reportable Range

We validated the method for the maximum values shown in the Linearity section. In principle, conventional HPGe instrumentation will be linear over a limitless range of activity concentrations. However, we may only report measurement values for activity concentrations within the range we have experimentally verified to be linear. Potentially, we may receive samples with activity concentrations higher than the maximum measurement values. In these instances, we may dilute the sample using deionized water to bring the activity concentration into the validated linearity range. During method validation, we diluted standard reference material to achieve target activity concentrations. The final analytical method, therefore, has been proven to be valid for the dilution factors used. We allow dilution factors for which the observed measurement accuracy was within 15% of reference value. The maximum dilution factors and the maximum reportable activity concentrations allowed are in Table 6.

### Specificity

Specificity is measuring only the correct component and is validated by examining the effects of potentially interfering substances on the measurement. (Division of Laboratory Sciences, 2020) We performed three separate investigations to search for possible interferences. The first was to test for possible interferences in 50 random and unique urine samples (see Table 7). The second was to search through a radionuclide database. The third was to investigate the potential for activity measurement interference due to the presence of an influencing radionuclide.

We searched a radionuclide database for gamma photon energies near those used to measure the activity of the analytes in this method ( $^{137}\text{Cs}$ ,  $^{60}\text{Co}$ ,  $^{131}\text{I}$ ,  $^{192}\text{Ir}$ ,  $^{75}\text{Se}$ , and  $^{99}\text{Mo}$ ). Isotope abundance plays a role in assessing the likelihood that the interfering radionuclide may appear in a sample. Another useful tool for determining the degree to which a neighboring peak may interfere with the peak used in the quantitation of one of the method analytes is the Resolution Factor (Gillings et al., 2020),  $R_s$ .

$$R_s = 1.18 \times \frac{E_{rb} - E_a}{FWHM_a + FWHM_b}$$

In the equation for  $R_s$ ,  $E_r$  is used for the energy of the peak for radionuclides a and b, respectively, as indicated by the subscript. The Full-Width Half-Maximum (Energy Resolution) is  $FWHM$  for radionuclides a and b, indicated by the subscript. Neighboring peaks with a value for  $R_s < 1$  indicate that the peaks may be possible interferences.

We assume that radionuclides of trace or unknown abundance are poor candidates to cause interference. Radionuclides with an unknown abundance or “trace” abundance are not good candidates to show up in a patient sample. Synthetically produced radionuclides are more likely to be present, but few of the synthetically produced possible interferences found in the database search are common enough to be considered a candidate to be an interfering radionuclide.

A high-activity radionuclide (not the measurement analyte) in the sample may influence counts in a peak used for quantitation of one of the method analytes. The mechanism for this occurring is via the Compton Scattering background. For example, in a measurement of  $^{137}\text{Cs}$ , the activity from present  $^{60}\text{Co}$  (gamma peak energies of 1173 and 1333 keV) may influence counts in the 661 keV  $^{137}\text{Cs}$  peak. The two  $^{60}\text{Co}$  peaks raise the Compton Scattering background over a continuum of lower energies. The 661 keV  $^{137}\text{Cs}$  peak falls in this range. Thus, in a solution containing only  $^{60}\text{Co}$  and no  $^{137}\text{Cs}$ , the spectrum analyzing software may report an activity for  $^{137}\text{Cs}$  that is higher than the  $^{137}\text{Cs}$  LOD that we have calculated. In such instances, we will manually inspect the spectrum to see if this is a “real” peak or due to Compton Scattering.

Analysis of samples where we measured for  $^{137}\text{Cs}$  in samples spiked with an influencing radionuclide ( $^{60}\text{Co}$ ,  $^{75}\text{Se}$ ,  $^{192}\text{Ir}$ , or Mo-99) shows a clear dependence of the  $^{137}\text{Cs}$  uncertainty on the activity of the influencing radionuclide. The average  $^{137}\text{Cs}$  measurement is mostly unaffected by influencing activity except in the case of  $^{60}\text{Co}$  as the influencing radionuclide.

We found no interferences in a set of measurements for 50 individual urine samples. The aggregate data indicate that analytes were not detectable in the set of individual urine samples.

The LARAWEB nuclide database from [nucleide.org](http://nucleide.org) (Bé and Bureau International des Poids et Mesures, 2013) was the source for our search for radionuclides with gamma peaks close

in energy to the gamma peaks of interest for  $^{137}\text{Cs}$ ,  $^{60}\text{Co}$ , and  $^{192}\text{Ir}$ . We found no significant risk of interference from such peaks.

We measured single radionuclide samples at varying activities for  $^{137}\text{Cs}$ ,  $^{60}\text{Co}$ ,  $^{192}\text{Ir}$ ,  $^{99}\text{Mo}$ , and  $^{75}\text{Se}$ . We compared the relationship of  $^{137}\text{Cs}$  activity to the activity of the influencing radionuclide. These measurements show that activity due to the influencing radionuclides can result in measurements of  $^{137}\text{Cs}$  that are higher than the LOD for  $^{137}\text{Cs}$ .

Activity in the influencing radionuclide results in deformations to the background, over which the  $^{137}\text{Cs}$  661 keV peak is found. The deformations raise the likelihood that the software mistakenly attributes background counts to  $^{137}\text{Cs}$  activity. We anticipate that a similar effect can be found in the measurements of samples not containing  $^{192}\text{Ir}$  but containing an influencing radionuclide. However, because the  $^{60}\text{Co}$  peaks are at high energy, influencing radionuclides may not deform the background enough for this effect to be visible in samples not containing  $^{60}\text{Co}$ .

The variance of the counts in the 661 keV peak rises with the activity of the influencing radionuclide. However, the average  $^{137}\text{Cs}$  activity measurement has only a slight dependence (in the case of  $^{60}\text{Co}$ , Figure 4) or no dependence on the activity of the influencing radionuclide. These effects are visible in Figure 4, which are plots of individual measurements for  $^{137}\text{Cs}$  activity concentration at the time of measurement (non-decay corrected) versus the activity concentration at the time of measurement of the influencing radionuclide.

The effect of the influencing radionuclide's activity upon the uncertainty of blank  $^{137}\text{Cs}$  measurements is visible in a plot of the average measured influencing radionuclide activity versus the  $^{137}\text{Cs}$  standard deviation (Figure 5). The plots include best-fit curves from the regression analyses. The fourth-order polynomial curves fit the data (Equation 9); they are linear on the y-axis and logarithmic on the x-axis.

$$y = \sum_{i=0}^4 a_i (\log_{10} x)^i \quad 6$$

## Stability

We assessed the stability of the analyte by performing a series of tests that mimiced the changes in handling and storage conditions of a sample of patient urine. These tests ensured that the measurement of the radionuclide activity concentration was not altered by the changes in conditions that may occur during shipping, receiving, preparation, and analysis. We measured two samples a total of three times before and after a change in handling and storage conditions and then compared the results. The conditions were short-term room temperature storage, long-term freezer storage at a specified temperature, and at least three freeze-thaw cycles. We observed no significant changes to radionuclide measurement.

## Robustness

Robustness is the capacity of the method to remain unaffected by small, deliberate variations. It is a measurement of the reliability of the method. The experimental parameters of count time, high voltage (or bias voltage), sample volume, and baseline restorer were varied deliberately within 20% of the adopted values. Measurements of prepared samples of  $^{137}\text{Cs}$ ,  $^{60}\text{Co}$ , and  $^{192}\text{Ir}$  with the varied parameters showed that analysis results are not substantially affected by the variation in count time and sample volume. High voltage variation did produce inaccurate results.

The adopted value for the sample count time is 900 seconds. The value was varied by  $\pm 20\%$  to obtain measurements in samples for each radionuclide ( $^{137}\text{Cs}$ ,  $^{60}\text{Co}$ , and  $^{192}\text{Ir}$ ) and at a variety of activity levels. The most substantial variation in measurements with a change of count time appeared in the samples containing  $^{192}\text{Ir}$ , which is on the order of 4%. The measurements agree within the method's precision uncertainty for  $^{137}\text{Cs}$ ,  $^{60}\text{Co}$ , and  $^{192}\text{Ir}$ .

We varied the high voltage by  $\pm 10\%$  or  $\pm 20\%$ . A +20% variation in the test for  $^{192}\text{Ir}$  gave a measurement with an unacceptable bias (-37%). At  $\pm 10\%$  variation, there was no significant difference in measurements for  $^{137}\text{Cs}$  and  $^{60}\text{Co}$ . In principle, when the HPGe measurement system meets quality assurance and quality control checks, the high voltage should not be changed nor be allowed to be changed accidentally. However, in rare instances, the only troubleshooting measure that manages to restore an out-of-control measurement system back into working order may be a slight alteration in high voltage. In these instances, we may rely upon these validation data to guide decisions, in consultation with the manufacturer's service engineers, about whether or not to shutdown a detector for repair service or to continue processing patient samples.

Sample Volume refers to the amount of sample contained in the 15 mL centrifuge tube placed inside the HPGe well for activity measurement and radionuclide identification and quantification. The efficiency calibration curve itself is sensitive to changes in the sample geometry because the efficiency is known to be dependent on the distance between the decaying radioactive source particle within the source matrix and the active detector volume. These sample geometry changes may include the shape or material of the sample container, the sample matrix, and the total amount of sample.

The most applicable variation in the sample geometry for this method is to the sample volume since there is a potential that less than 10 mL (adopted sample volume) of a patient urine sample is received. We compared results for sample volumes of 5, 8, 10, 12, and 15 mL (see Tables 8 and 9).

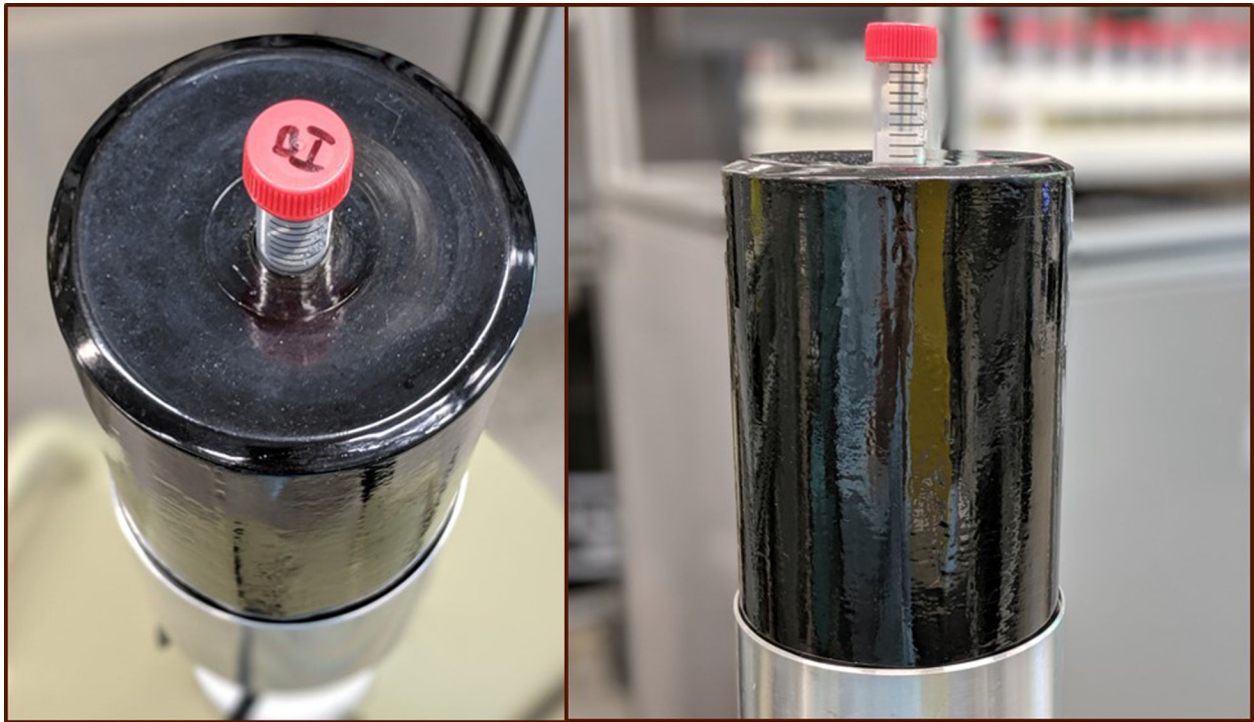
## Conclusions

We successfully validated the rapid gamma bioassay analytical method according to our laboratory policy, FDA Guidance, and CLIA specifications and regulations. The method is valid for the measurement of single radionuclide samples of patient urine. CDC will use this method to assess internal radionuclide contamination in individuals following a radiological or nuclear emergency or incident. We have the ability to measure contamination far below

the NCRP CDG levels for  $^{137}\text{Cs}$ ,  $^{60}\text{Co}$ , and  $^{192}\text{Ir}$ . Further method development and validation work are necessary to prove accuracy, precision, and LOD sensitivity of the method for specific multi-radionuclide scenarios. With significantly increased count time, we may use a modified version of this method for studies monitoring radionuclide activity concentrations in the general population.

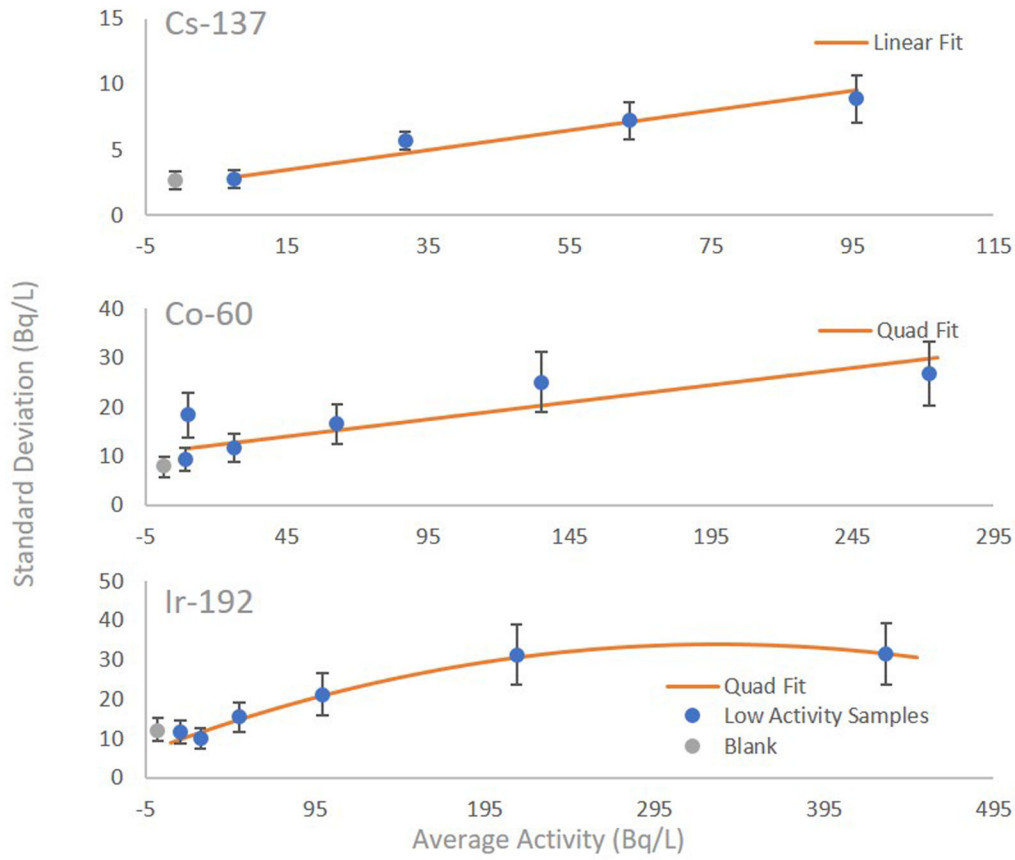
## References

- Bé M-M, Bureau International des Poids et Mesures (Eds.), 2013. Table of radionuclides. Vol. 7: A=14 to 245, Monographie BIPM. BIPM, Sèvres.
- Blaauw M, 1993. The use of sources emitting coincident  $\gamma$ -rays for determination of absolute efficiency curves of highly efficient Ge detectors. Nuclear Instruments and Methods in Physics Research Section A: Accelerators, Spectrometers, Detectors and Associated Equipment 332, 493–500. 10.1016/0168-9002(93)90305-2
- Center for Drug Evaluation and Research, Center for Veterinary Medicine, 2018. Bioanalytical Method Validation Guidance for Industry.
- CLSI, 2012. Evaluation of Detection Capability for Clinical Laboratory Measurements Procedures; Approved Guideline - Second Edition.
- Division of Laboratory Science (Ed.), 2020. DLS Policies and Procedures Manual (Version 7.0).
- Dörr HD, Meineke V, 2006. Appropriate radiation accident medical management: necessity of extensive preparatory planning. Radiation and Environmental Biophysics 45, 237–244. 10.1007/s00411-006-0068-x [PubMed: 17047978]
- E. Toohey R, 2003. Internal dose assessment in radiation accidents. Radiation Protection Dosimetry 105, 329–331. 10.1093/oxfordjournals.rpd.a006250 [PubMed: 14526980]
- Gelsema SJ, 2001. Advanced [ $\gamma$ ]-ray spectrometry dealing with coincidence and attenuation effects: a three curves approach. DUP Science, Delft.
- Gillings N, Todde S, Behe M, Decristoforo C, Elsinga P, Ferrari V, Hjelstuen O, Peitl PK, Koziorowski J, Laverman P, Mindt TL, Ocak M, Patt M, 2020. EANM guideline on the validation of analytical methods for radiopharmaceuticals. EJNMMI radiopharm. chem. 5, 7. 10.1186/s41181-019-0086-z
- Gunnink R, Prindle AL, 1992. Nonconventional methods for accurately calibrating germanium detectors. Journal of Radioanalytical and Nuclear Chemistry Articles 160, 305–314. 10.1007/BF02037106
- Keith S, Murray HE, Spoo W, 1999. Toxicological Profile for Ionizing Radiation.
- National Council on Radiation Protection and Measurements (Ed.), 2009. Management of persons contaminated with radionuclides: handbook: recommendations of the National Council on Radiation Protection and Measurements, 12 20, 2008, NCRP report. National Council on Radiation Protection and Measurements, Bethesda, Md.
- Obodovskiy I, 2015. Fundamentals of radiation and chemical safety. Elsevier, Amsterdam ; Boston.
- ORTEC, 2017. GammaVision (R) Gamma-Ray Spectrum Analysis and MCA Emulator for Microsoft(R) Windows(R) 7, 8.1, and 10 Professional (A66-BW Software User's Manual Software Version 8.1) Manual Revision L.
- Schull WJ, Weiss KM, 1992. Radiation Carcinogenesis in Humans, in: Advances in Radiation Biology. Elsevier, pp. 215–258. 10.1016/B978-0-12-035416-0.50015-X
- Taylor JK, 1987. Quality assurance of chemical measurements. Lewis Publishers, Chelsea, Mich.

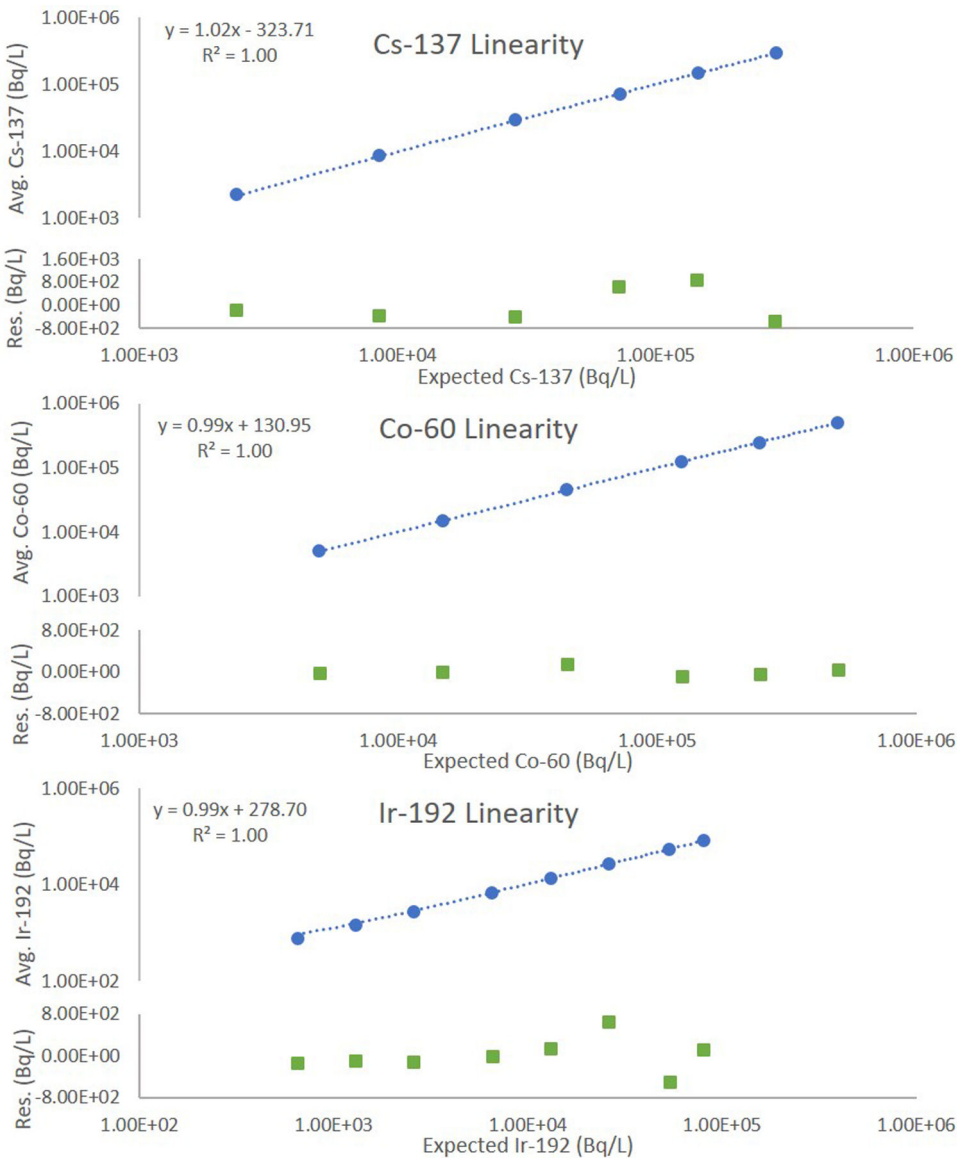


**Figure 1.**

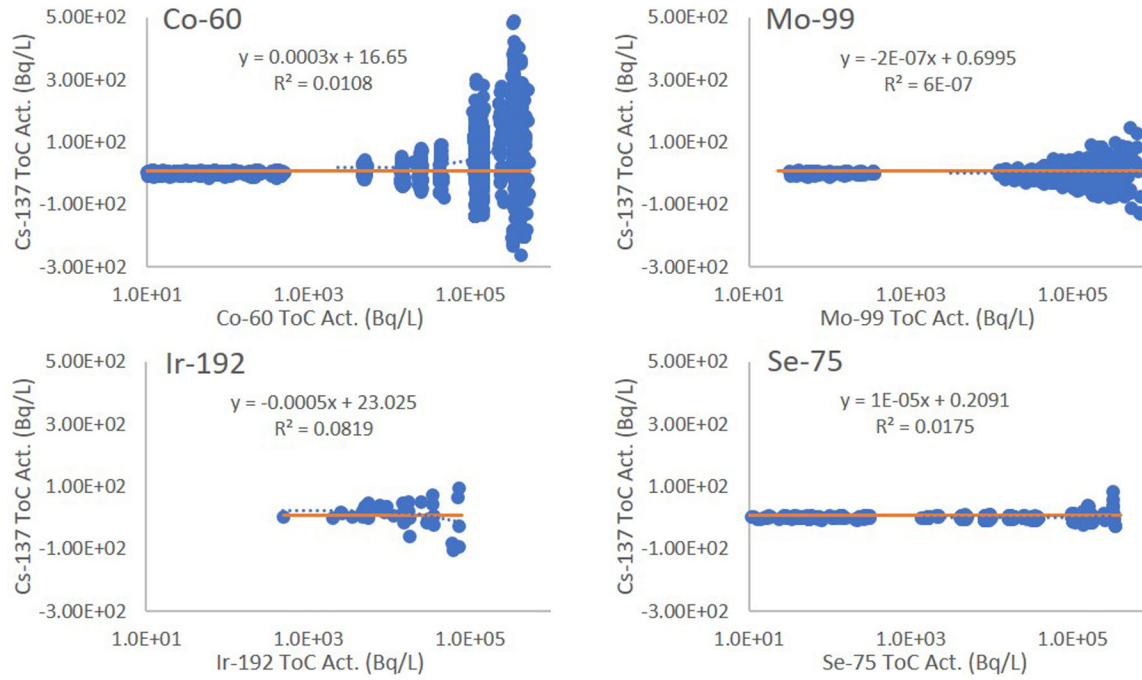
Top and side views of an HPGe p-type reverse coaxial well detector with carbon fiber endcap: The detector is outside of its sample changer cabinet and lead shield. A 15-mL polypropylene centrifuge tube is in the well of the detector.

**Figure 2.**

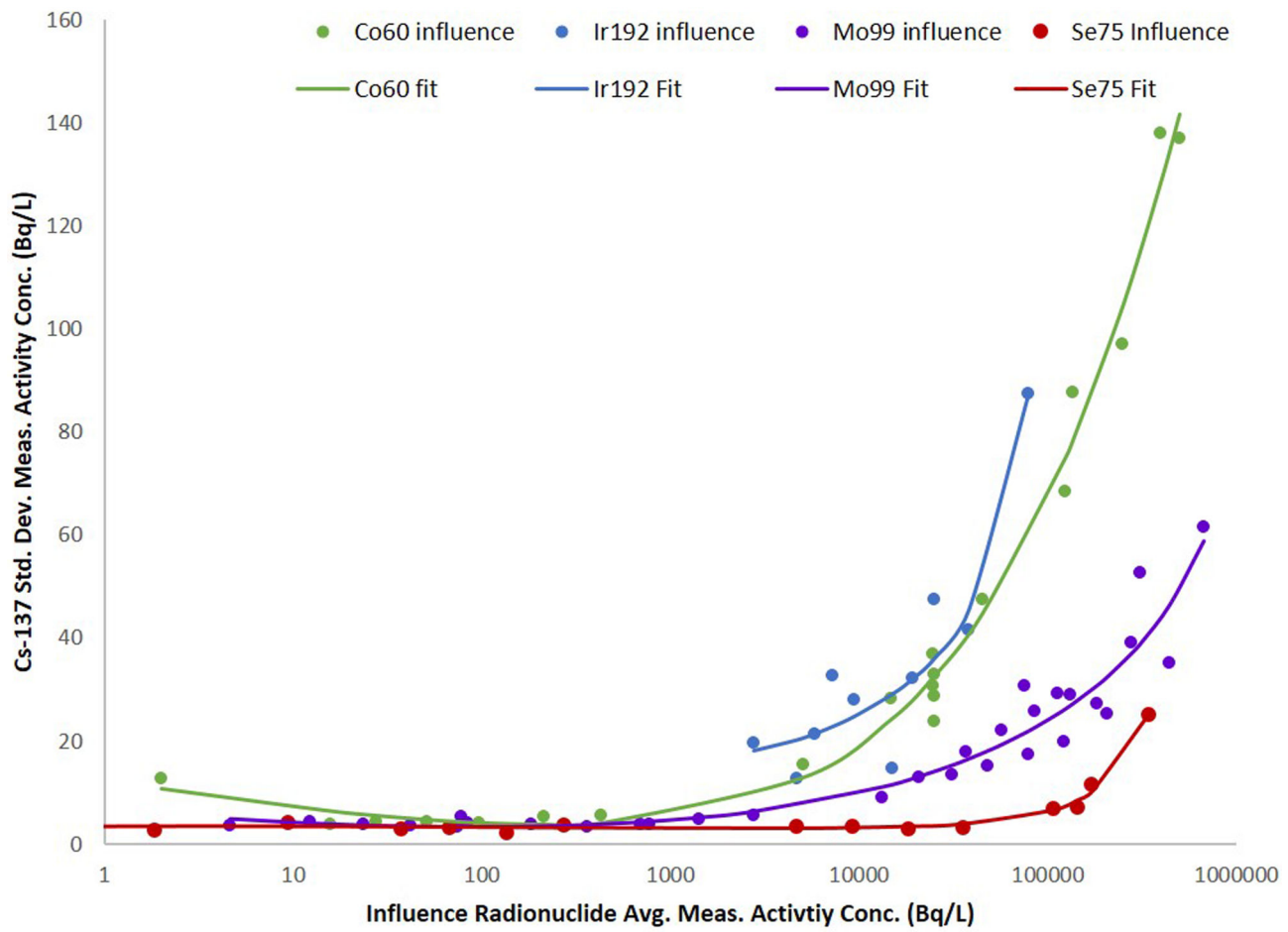
The standard deviation vs. average activity concentration measurement is used for calculating the Limit of Detection (LOD) for  $^{137}\text{Cs}$ ,  $^{60}\text{Co}$ , and  $^{192}\text{Ir}$ . The low activity sample measurements are BLUE circles with error bars, which are related to the number of measurements. The ORANGE line is the best fit through the low activity sample data. The legend indicates the fit model used (quadratic or linear), and the measurement data for each blank sample are GREY circles.

**Figure 3.**

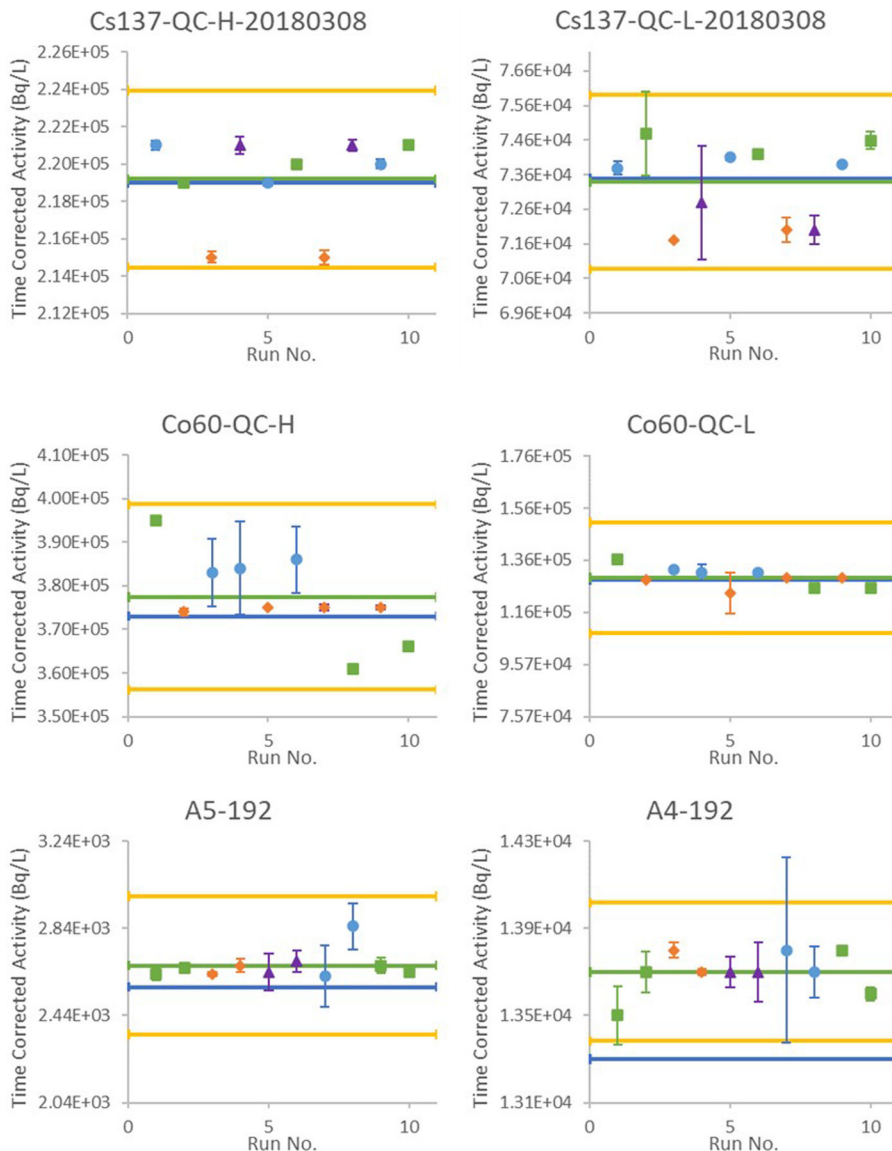
Plots of linearity data for  $^{137}\text{Cs}$  (TOP),  $^{60}\text{Co}$  (MIDDLE), and  $^{192}\text{Ir}$  (BOTTOM). For each radionuclide, the average measurements vs. expected measurements are shown (blue circles) along with a linear fit through the data (dashed line). We show the fit equation and the associated coefficient of determination  $R^2$  for each fit. The residual vs. expected data (green squares) does not have a curvilinear relationship.

**Figure 4.**

Influence of  $^{60}\text{Co}$  activity on the measurement of  $^{137}\text{Cs}$ . Samples are spiked with  $^{60}\text{Co}$  and are blank for  $^{137}\text{Cs}$ . The ORANGE line is the  $^{137}\text{Cs}$  LOD (7.2 Bq/L), obtained from the comparison of  $^{137}\text{Cs}$  measurements of blank samples and low-activity level samples.

**Figure 5.**

Plot of the average measured activity concentration in Bq/L for each of the influencing radionuclides versus the standard deviation of the blank or background  $^{137}\text{Cs}$  measurement. DOTS represent the average measurements data, and SOLID LINES represent the best-fit curves for each radionuclide. The fit is a fourth-order polynomial of the log X-lin Y plot.

**Figure 6.**

Precision data with the target value (blue line), mean measurement (green line),  $\pm 2\sigma$  standard deviation (yellow lines), run mean measurement (blue data points), within-run standard deviation (error bars). The data is shown for three analytes ( $^{137}\text{Cs}$ ,  $^{60}\text{Co}$ , and  $^{192}\text{Ir}$ ) and at two activity levels. Each data point color and shape represents one of four instrument systems.

**Table 1:**

Clinical Decision Guide (CDG) level in Children or Pregnant Women (C/P) for a sample collected 1 or 5 day(s) following an acute radiological contamination incident. The Limits of Detection (LOD) for this method are lower than the CDG values by orders of magnitude.

Nuclide	LOD (Bq/L)	CDG C/P Day 1 Post Exposure (Bq/L)	CDG C/P Day 5 Post Exposure (Bq/L)
<sup>60</sup> Co	45.7	1.19E+04	1.00E+03
<sup>137</sup> Cs	7.2	1.77E+05	2.90E+04
<sup>131</sup> I	16.8	6.46E+03	2.00E+00
<sup>192</sup> Ir	36.6	2.64E+03	1.90E+02
<sup>99</sup> Mo	19.2	TBD	TBD
<sup>75</sup> Se	13.7	TBD	TBD

**Table 2:**

Certified activity values for the TCC mixture calibrator solution (EZAG SRS#114539). The certificate reference date is 8/1/2019 12:00:00 PM. Peak energies for which cascade summing affects radionuclide analysis are in italics.

Radionuclide	Full-Energy Peak (keV)	Branching Ratio (%)	Half-life (days)	Activity (Bq)	Gammas per second	Activity Uncertainty (%)
<sup>241</sup> Am	59.54	35.92	1.58E+05	481.75	172.95	2
<sup>109</sup> Cd	88.03	3.66	4.61E+02	4348.43	160.93	3.5
<sup>57</sup> Co	<i>122.07</i>	<i>85.6</i>	<i>2.72E+02</i>	<i>112.82</i>	<i>96.57</i>	<i>1.8</i>
<sup>139</sup> Ce	<i>165.86</i>	<i>79.9</i>	<i>1.38E+02</i>	<i>154.41</i>	<i>123.53</i>	<i>2.1</i>
<sup>203</sup> Hg	279.2	81.48	4.66E+01	363.38	296.34	1.8
<sup>113</sup> Sn	391.7	64.97	1.15E+02	243.19	157.99	1.8
<sup>134</sup> Cs	<i>604.72</i>	<i>97.62</i>	<i>7.54E+02</i>	<i>540.74</i>	<i>527.85</i>	<i>1.8</i>
<sup>134</sup> Cs	<i>795.86</i>	<i>85.46</i>	<i>7.54E+02</i>	<i>129.25</i>	<i>109.98</i>	<i>1.8</i>
<sup>137</sup> Cs	661.66	84.99	1.10E+04	540.74	462.22	1.8
<sup>54</sup> Mn	834.85	99.97	3.12E+02	306.20	306.20	1.4
<sup>88</sup> Y	<i>898.04</i>	<i>93.7</i>	<i>1.07E+02</i>	<i>561.47</i>	<i>526.24</i>	<i>1.4</i>
<sup>65</sup> Zn	1115.54	50.22	2.44E+02	817.14	408.87	1.4
<sup>88</sup> Y	<i>1836.06</i>	<i>99.35</i>	<i>1.07E+02</i>	<i>561.47</i>	<i>557.04</i>	<i>1.8</i>

**Table 3**

Standard source solution data: Source suppliers are Eckert & Ziegler Analytics (EZAG), National Institute of Standards and Technology (NIST), and Eckert & Ziegler Isotope Products (ZIP). The preparation column has acid concentration data. The supplier provides an estimate of the relative expanded uncertainty ( $k=2$ ) for each reference activity, shown as U (%).

Analyte	Supplier	Certification Number	Reference Date	Preparation	Reference Activity (Bq/L)	Uncertainty (%)
$^{137}\text{Cs}$	EZAG	106645	7/19/2017	0.1 M HCl	3.72E+07	1.8
$^{60}\text{Co}$	NIST	$^{60}\text{Co}$ ICLN/DHS RDD	12/31/2007	1.1 M HCl	3.35E+06	3.0
$^{192}\text{Ir}$	EZIP	1984-7	10/15/2017	0.1 M HCl	1.71E+08	3.0

**Table 4**

Accuracy Data for  $^{137}\text{Cs}$ ,  $^{60}\text{Co}$ , and  $^{192}\text{Ir}$  HPGe method at three reference value levels for each analyte. The Approximate CDG Equivalent column compares the 5- or 1-day CDG level with the reference value (Table 1). The mean is the average measurement over 10 analytical runs with one measurement per run. The difference from the reference value column compares the mean value and the reference value. The z-score column also makes this comparison but includes the uncertainties of the reference and the measurement values.

Analyte	Approx. CDG Equiv.	Reference Value (Bq/L)	Observed Mean Value (Bq/L)	SD (Bq/L)	Diff. from Ref. (%)	Z-score
$^{137}\text{Cs}$	$\frac{1}{3}\times \text{C/P}$ (5 day)	(8.46±0.16)E+03	(8.66±0.23)E+03	2.21E+02	2.30	0.69
	1x Adult (5 day)	(1.45±0.03)E+05	(1.47±0.05)E+05	4.28E+03	1.40	0.39
	2x Adult (5 day)	(2.90±0.05)E+05	(2.96±0.13)E+05	1.18E+04	2.28	0.49
$^{60}\text{Co}$	1x Adult (5 day)	(4.97±0.06)E+03	(5.04±0.18)E+03	1.31E+02	1.45	0.37
	1x Adult (1 day)	(4.50±0.05)E+04	(4.47±0.16)E+04	1.08E+03	-0.61	-0.18
	8x Adult (1 day)	(5.01±0.05)E+05	(4.98±0.31)E+05	2.91E+04	-0.64	-0.10
$^{192}\text{Ir}$	1x C/P (1 day)	(2.58±0.08)E+03	(2.75±0.14)E+03	1.37E+02	5.69	1.05
	2x Adult (1 day)	(2.60±0.08)E+04	(2.68±0.05)E+04	4.33E+02	1.85	0.85
	4x Adult (1 day)	(5.33±0.16)E+04	(5.33±0.07)E+04	4.99E+02	-0.96	0.00

**Table 5**

Precision Data for HPGe measurements of  $^{137}\text{Cs}$ ,  $^{60}\text{Co}$ , and  $^{192}\text{Ir}$  at two activity levels. The within-run relative standard deviation compares two individual measurements within a run to the mean value for that run, while the between-run relative standard deviation compares the mean measurement from a single run to the mean measurement shown in the table. Summing the within- and between-run relative standard deviations in quadrature yields the total.

Analyte	Sample No.	Mean Measurement (Bq/L)	Relative Standard Deviation (%)		
			Within Run	Between Run	TOTAL
$^{137}\text{Cs}$	1	2.19E+05	0.13	1.08	1.09
	2	7.34E+04	0.92	1.45	1.71
$^{60}\text{Co}$	1	3.77E+05	1.29	2.51	2.82
	2	1.29E+05	2.09	2.49	3.25
$^{192}\text{Ir}$	1	1.38E+04	1.15	--	1.15
	2	2.67E+03	2.49	1.81	3.07

**Table 6**

The maximum activity concentration (Bq/L) for which we have validated linearity for each radionuclide. We calculate the maximum reportable activity concentration (Bq/L) from the maximum linear measurement by multiplying by the maximum allowed dilution factor.

Nuclide	Max Linear Range (Bq/L)	Max Dilution Factor	Max Reportable (Bq/L)
<sup>137</sup> Cs	2.90E+05	4340	1.26E+09
<sup>60</sup> Co	5.01E+05	168	8.42E+07
<sup>192</sup> Ir	8.09E+04	31962	2.59E+09

**Table 7**

Aggregate data from 50 individual urine sample measurements. These measurements do not exceed the calculated LOD value.

Nuclide	LOD (Bq/L)	Average Ind. Urine Meas. (Bq/L)	2 $\sigma$ Ind. Urine Meas. (Bq/L)
$^{60}\text{Co}$	45.7	0.9	4.4
$^{137}\text{Cs}$	7.2	1.0	3.1
$^{192}\text{Ir}$	36.7	5.9	13.1

**Table 8**

Sample Volume variation effect on the measurement of  $^{192}\text{Ir}$  at two activity concentration levels

Sample Volume (mL)	Parameter Change	Measurement (Bq/L)	Diff	Test Date	Test Detector
10	adopted	1.90E+04		3/24/2020	MCB 134
5	-50%	1.87E+04	-2%	3/13/2020	MCB 133
8	-20%	2.00E+04	5%	3/24/2020	MCB 134
12	20%	1.95E+04	3%	3/24/2020	MCB 134
15	50%	1.73E+04	-9%	3/13/2020	MCB 133

Sample Volume (mL)	Parameter Change	Measurement (Bq/L)	Diff	Test Date	Test Detector
10	adopted	6.06E+03		3/24/2020	MCB 134
5	-50%	5.64E+03	-2%	3/13/2020	MCB 133
8	-20%	6.13E+03	1%	3/24/2020	MCB 134
12	20%	5.83E+03	-4%	3/24/2020	MCB 134
15	50%	5.30E+03	-12%	3/13/2020	MCB 133

**Table 9**

Sample Volume variation effect on the measurement of  $^{60}\text{Co}$  at two activity concentration levels

Sample Volume (mL)	Parameter Change	Measurement (Bq/L)	Diff	Test Date	Test Detector
10	adopted	3.61E+05			
8	-20%	3.85E+05	7%	3/13/2020	MCB134
12	20%	3.19E+05	-12%		

Sample Volume (mL)	Parameter Change	Measurement (Bq/L)	Diff	Test Date	Test Detector
10	adopted	1.25E+05			
8	-20%	1.31E+05	5%	3/13/2020	MCB134
12	20%	1.15E+05	-8%		